Sensors & Actuators: B. Chemical 328 (2021) 129058

Contents lists available at ScienceDirect

Sensors and Actuators: B. Chemical

journal homepage: www.elsevier.com/locate/snb

Facile preparation of N-S co-doped graphene quantum dots (GQDs) from graphite waste for efficient humidity sensing

Khouloud Jlassi [a,*,1], Shoaib Mallick [b,1], Abubaker Eribi [c], Mohamed M. Chehimi [d], Zubair Ahmad [a,*], Farid Touati [b], Igor Krupa [a]

[a] Center for Advanced Materials (CAM), Qatar University, 2713 Doha, Qatar
[b] Department of Electrical Engineering, Qatar University, 2713 Doha, Qatar
[c] Department of Chemistry and Earth Sciences, Qatar University, 2713 Doha, Qatar
[d] Univ Paris Est, ICMPE (UMR7182), CNRS, UPEC, F-94320 Thiais, France

ARTICLE INFO

Keywords:
GQDs
Humidity sensor
Response and recovery times
Hysteresis

ABSTRACT

In this work, graphene quantum dots (GQDs) were prepared from Graphitic waste. The resulting GQDs were evaluated for the potential application for resistive humidity sensors. The resistive humidity sensors were fabricated on the pre-patterned interdigital ITO electrodes using the three different concentrations (2.5, 5.0, and 10 mg) of GQDs in DMF. The GQDs films were deposited using the spin coating technique. The GQDs (10 mg/ml) based impedance sensors showed good sensitivity and lowered hysteresis as compared to the other ratios (2.5 and 5 mg) of the GQDs. The maximum calculated hysteresis of the GQDs (10 mg) based humidity sensor is around 2.2 % at 30%RH, and the minimum calculated hysteresis of the GQDs (10 mg/ml) based humidity sensor is approximately 0.79 % at 60 %RH. The response and recovery time found to be 15 s and 55 s, respectively. The interesting humidity-dependent resistive properties of these prepared GQDs make them promising for potential application in humidity sensing.

1. Introduction

Typically, the humidity sensors are fabricated by utilizing a wide range of materials, such as; polymers [1], clays, and ceramics [2], nanomaterials [3], and hybrid composites [4] that functioned as active sensing films. Although composites layers predominantly comprised of hydrophobic polymers, and these sensing components detects humidity from their surrounding through the alteration of electrical conductivity upon adsorption of vapor molecules. Recently, carbon-based humidity sensors [5] have managed to capture substantial attention by their economical, easy-processing, and flexibility-accommodating attributes [6]. Among the different allotropes of carbon, graphene has attracted the attention of many researchers in the emergent materials field [7]. With the extraordinary chemical and physical properties such as excellent electrical and thermal conductivity, excellent resistance to corrosion and stability, high strength, graphene-based materials became the researcher's first choice when it comes to sensor fabrication [8].

Different dopants added to the graphene to support the alienation of adsorbed water into hydrogen and hydroxyl ions [9]. The bulk resistivity is decreased by the hydroxyl ions, which can later be considered as an AC impedance. The water, which is captivated into the film due to diffusion through the capillary or bulk transport of water into the film's pores, variations in conductance or capacitance, can be calculated. Improvement in humidity response measurements of the sensors has been observed using graphene quantum dots (GQDs), particularly in terms of sensitivity of the devices towards change in different relative humidity [10]. The term "graphene quantum dots (GQDs)" is used to describe the minuscule fragments, limited in size, or domains, of single-layer to tens of layers of graphene (the typical size of the most of the GQDs is in the range of 3-20 nm). The shape of most GQDs is circular & elliptical, but there are triangular, quadrate, and hexagonal dots as well [11]. Their reduced size induces a shift of the electronic excitations to higher energy, concentrating the oscillator strength into just a few transitions, conferring unique quantum-confined photonic and electronic properties. Quantum dots based materials have been widely used in different domains; biomedical [12], agriculture [13], energy conversion [14], optoelectronics [15], and more recently in sensing applications [16,17]. However, quantum dots materials were found to be

* Corresponding authors.
E-mail addresses: Khouloud.jlassi@qu.edu.qa (K. Jlassi), zubairtarar@qu.edu.qa (Z. Ahmad).
[1] Khouloud Jlassi and Shoaib Mallick contributed equally.

https://doi.org/10.1016/j.snb.2020.129058
Received 29 May 2020; Received in revised form 11 October 2020; Accepted 16 October 2020
Available online 22 October 2020

very toxic [18,19] and relatively expensive. Therefore, researchers are more interested nowadays in developing suitable low cost and non-toxic alternatives, namely carbon and graphene quantum dots (GQDs). The GQDs latter's attracted many researchers because of their unique and outstanding properties such as easy preparation [20], low cost, and toxicity [21,22], photoluminescence, and bandgaps [23,24]. GQDs have been prepared by a different route, mainly by chemical [25], ultrasonic-assisted [26], microwave-assisted [27], plasma-assisted, and laser-assisted methods [28]. These methods use expensive carbon sources such as carbon nanotubes [29] and carbon nanofiber [30], however more recently, the trends are using lost cost carbon sources, especially carbon wastes materials, to prepare (GQDs) for added value applications [31].

In this work, we describe a cost-effective and facile way to prepare highly photoluminescent GQDs, using graphite waste as a carbon source. The morphology and physio-chemical properties of the obtained GQDs were assessed by X-ray photoelectron (XPS), Raman, Fourier-transform infrared (FTIR), X-ray diffraction (XRD), atomic force microscopy (AFM), and electron microscopy (SEM and TEM). The optical properties were explored using Fluorescence and U.V./Vis spectroscopy (U.V./Vis). The hydrophilicity of GQDs based sensing film is studied by the contact angle measurement method. Interestingly, it is observed that the concentrations of GQDs can alter the wettability of the sensing film. The resulting GQDs based sensors were evaluated as a novel low-cost impedance humidity sensor.

2. Experimental

2.1. Materials and chemicals

Graphite wastes were obtained from Qatalum (Doha, Qatar). Sulfuric acid (99.9%), nitric acid (70%), ammonia (99.9%), and sodium hydroxide (99.9%) were obtained from Aldrich.

2.2. Synthesis and purification of GQDs

4 g of graphite waste in powder form was first dissolved in H_2SO_4/HNO_3 (200/60 ml) for 12 h and at 120 °C; after that, diluted and neutralized using ammonia as following, 10 ml of the material was dissolved in water (0.1 mg/mL) under vigorous stirring, then mixed with 3 ml of ammonia and sonicated for 20 min; the resulting material was then heated at 180̊ C for 12 h using an autoclave. The supernatant was then filtered then dialyzed (3500 Da MWCO) membranes, yielding a deep yellow supernatant N-GQDs.

2.3. Preparation of humidity sensor based GQDs

Three different concentrations of GQDs (2.5, 5, and 10 mg) solutions were prepared by dispersing in DMF. The GQDs solution is deposited on the ITO/glass electrode substrate by using a spin coating technique. The interdigitated ITO electrodes (S161) were purchased from Ossila UK. The thickness of ITO on the glass substrate was 100 nm., The dimensions of the substrates were (20 mm x 15 mm). It consists of the 5 ITO based interdigitated electrodes, while each interdigitated electrode consists of three channels with a dimension of 30 mm x50 µm. First, the ITO electrodes were cleaned for 10 min, under sonication, and using soap water then washed by distilled water. After that, the ITO electrodes were sonicated in acetone, distilled water for 10 min each, and then dried under nitrogen gas. During the deposition of sensing film, an optimization process was conducted for rotation speed and rotation time to achieve an even equilateral distribution of the solution. The rotation speed and rotation time was set to 5000 rpm and 50 seconds. Fig. 1 (a) shows a graphical presentation of the preparation process of the GQDs based humidity sensor. The humidity sensing response of GQDs based impedance sensors was carried out in a controlled humidity chamber. The humidifier (model HM3000) was used to increase the humidity level inside the sealed humidity chamber. The Drierite based desiccant was connected to the humidity chamber through an inlet valve to decrease the humidity level inside the chamber. The RS-6109 humidity meter was used as a reference humidity sensor placed inside the humidity chamber to observe the humidity level. The impedance response of the GQDs based humidity sensor was measured by MS5308 LCR meter. Fig. 1 (b) demonstrates the humidity sensing measurement setup used in this study.

Here it is important to note that We performed our experiment within the sealed chamber, where ambient air was used to increase and decrease the relative humidity levels. A humidifier has been connected to the sealed chamber by an inlet valve, which flows humid air into the sealed chamber to raise the moisture levels. Drierite based desiccant was to circulate the moist air to reduce the humidity level within the sealed chamber. As the scope of this study was limited to the test the explore the potential of the N-S co-doped graphene quantum dots (GQDs) for the humidity sensing in the open atmosphere, hence we did not perform the cross-sensitivity of the different gases in this work.

2.4. Characterization

To track the morphological changes of used materials and sensing films, scanning electron microscopy (SEM, FEI NOVA Nano-450, and the Netherlands), transmission electron microscopy (TEM, FEI, TALOS

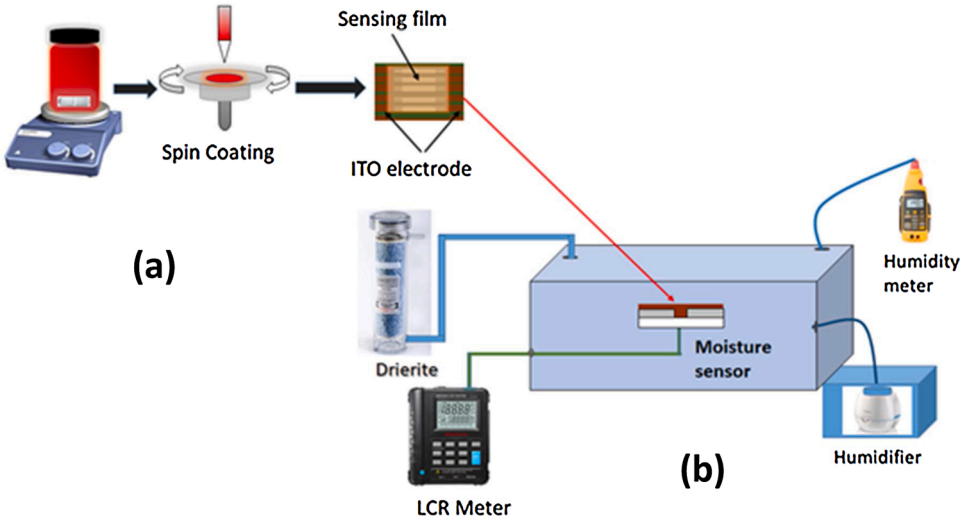

Fig. 1. (a) Schematic presentation of GQDs based humidity sensor fabricated by the spin coating method. (b) A humidity sensor setup was used during this work.

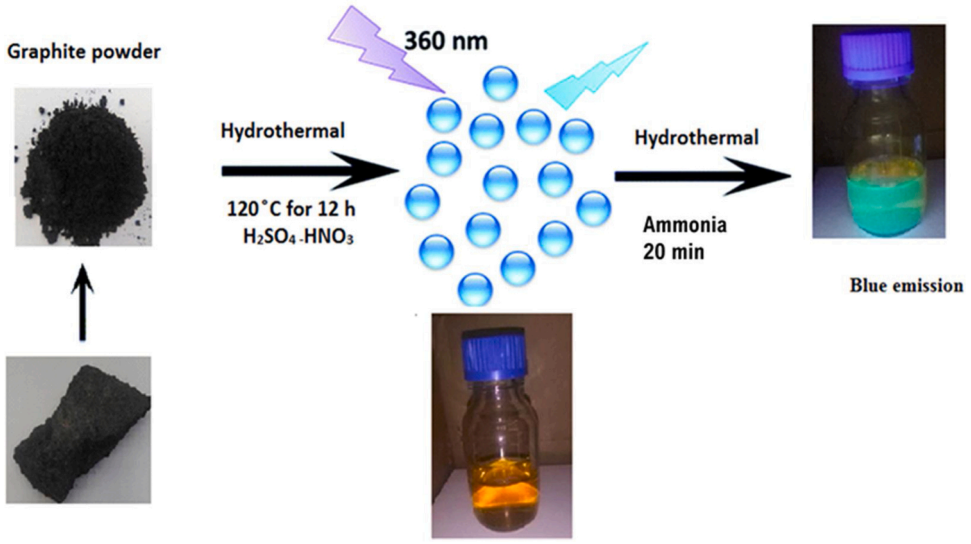

Fig. 2. Schematic illustration summarizing the preparation of N and S co-doped GQDs from graphite waste.

F200X, USA), and atomic force microscopy (AFM, MFP-3D, Asylum Research, USA) machine, were used. The X-ray diffraction (XRD) measurements were performed using a PANalytical instrument (model X'PertPRO) with Co Kα (1.789 Å) radiation. FTIR analysis was carried out using the FTIR Frontier (Perkin Elmer, Frontier, USA) instrument, from (4000 to 500 cm^{-1}). X-ray photoelectron spectra (XPS) were obtained using an Axis Ultra apparatus (Kratos, Manchester, UK) instrument fitted with a monochromatic Al Kα X-ray source. Water drop contact angles were measured Data physics apparatus (OCA 35, Germany); the drop volume was 5 µL. Characterization. To track the optical properties, sample characterization was carried out on a Shimadzu UV-3600 spectrophotometer, FLS920 P fluorescence spectrometer (Edinburgh Instruments), PL decays were recorded using picosecond pulsed diode lasers (Edinburgh Instruments EPLED-320 320 nm, 5 mW and EPL-405 405 nm, 5 mW). The decay data were deconvoluted with the instrument response function and fitted with a multiexponential fit to derive fluorescence lifetimes by taking the weighted average of exponential components. An integrating sphere from Edinburgh Instruments was used to measure the absolute PL QYs.

3. Results and discussion

3.1. Synthesis and purification of GQDs from graphite waste

Graphite wastes were collected from the Qatalum Qatar industry then crushed to obtain a fine powder. The latter was then dispersed into concentrated H_2SO_4/ HNO_3 solution under sonication, then heated under constant stirring at 120̊ C for 12 h. After cooling at room temperature, the resulting mixture was, filtered, diluted, and then dialyzed. A GQDs solution with yellowish color was acquired, displaying green

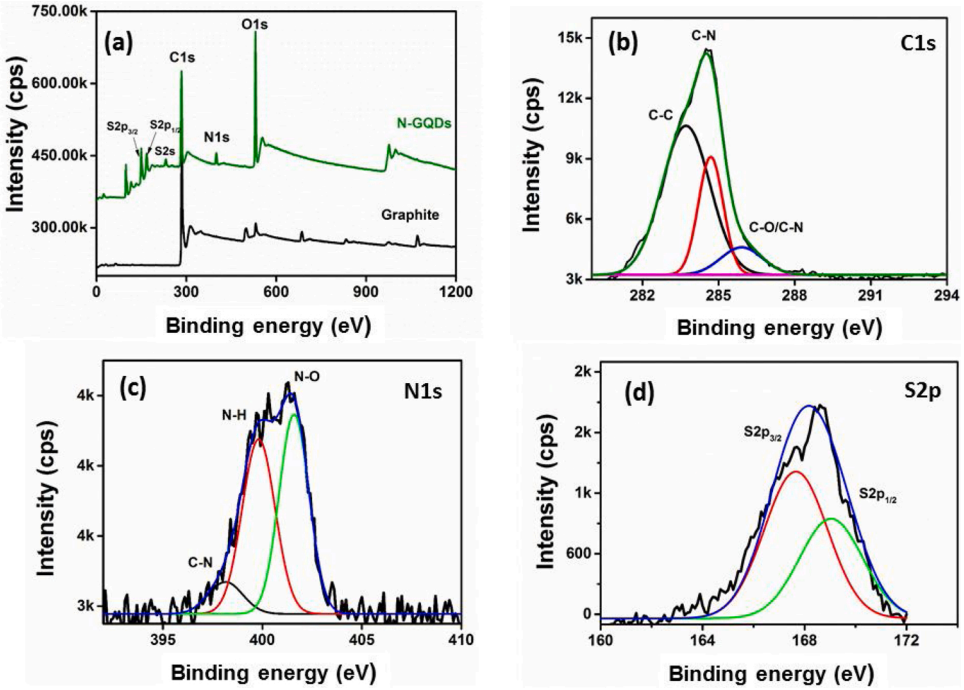

Fig. 3. XPS survey regions of Graphite waste, N-GQDs, high-resolution (b) C1 s, (c) N1 s region, and (d) S2p of the obtained N-GQDs.

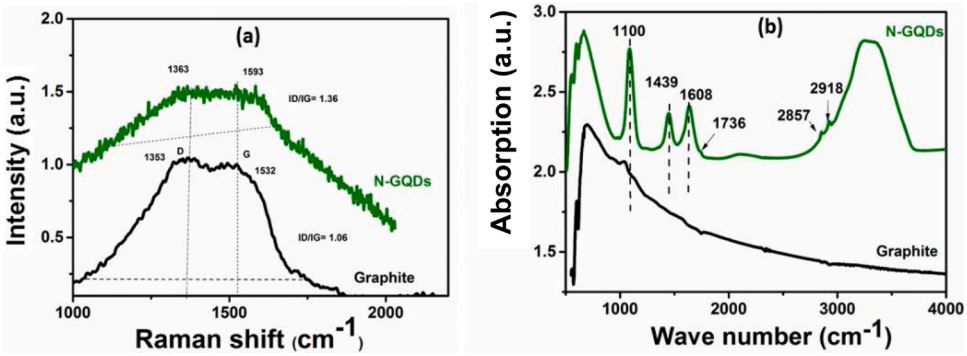

Fig. 4. Raman spectra (a) and FTIR spectra (b) of graphite waste and N-GQDs derivate.

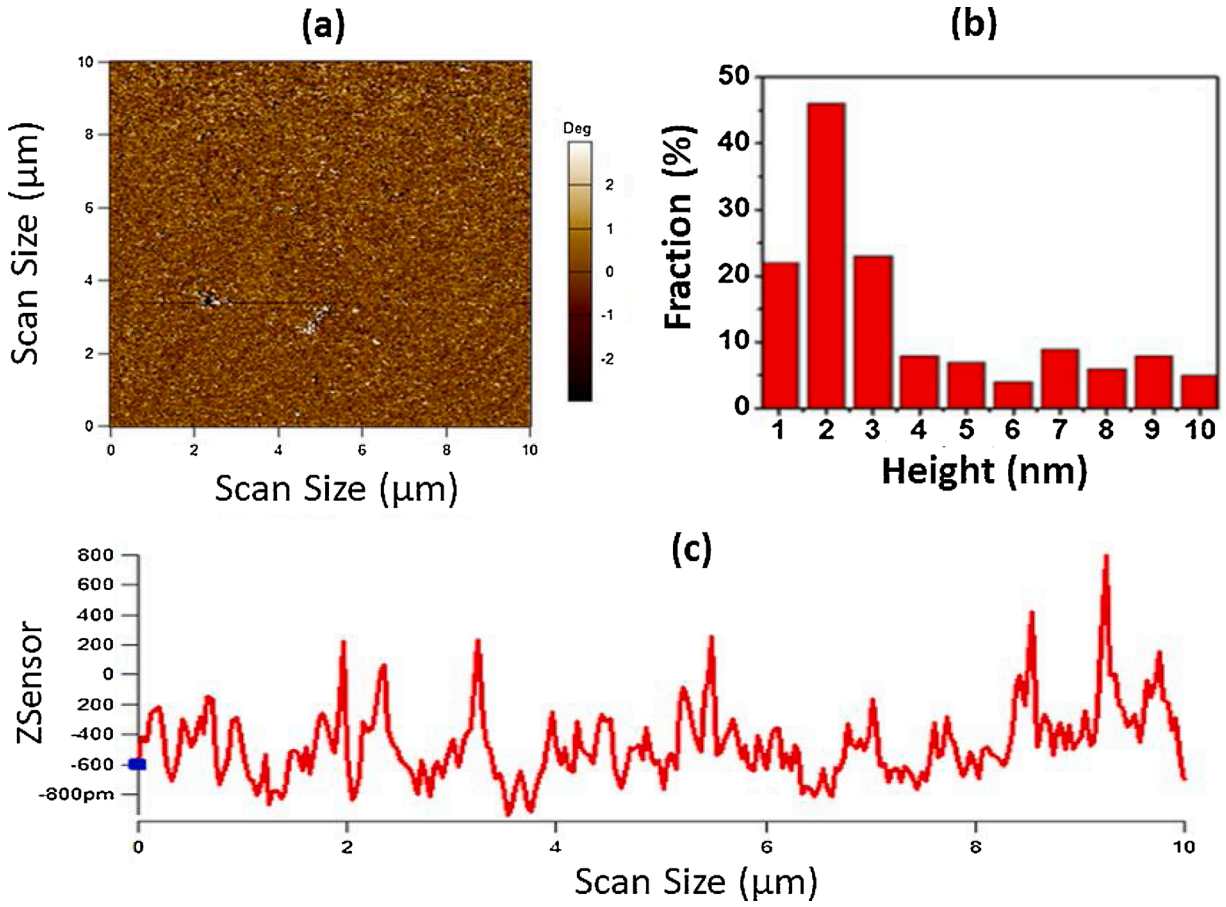

Fig. 5. AFM image (a), the height distribution (c), and the height profile is corresponding to the AFM image (b) of N-GQDs from graphite waste on the ITO glass substrate.

emission under UV light (360 nm).

The as-prepared GQDs material was then treated with ammonia for 20 min using a hydrothermal process to obtain N and S co-doped GQDs, yielding a deep yellow solution, with a blue-green emission when excited at 365 nm UV light, as shown in Fig. 2.

3.2. Chemical structure of Graphite waste and the prepared N-GQDs

The surface chemical composition of the graphite waste and the as-prepared GQDs was explored first using the XPS surface analysis technique. As shown in the XPS general survey (Fig. 3.a), one can note the presence of C1 s and O1 s only for the graphite sample. However, the prepared GQDs showed N1 s, S2p, C1 s, and O1 s, indicating the successful formation of GQDs enriched with N and S; moreover, a significant increase was noted in both C1 s and O1 s peaks of GQDs compared of graphite waste, confirming the high oxidation degree of the carbon surface. The C1 s XPS high-resolution spectra of the N-GQDs, shown in (Fig. 3.b), can be fitted as follows; C-C at 284.9 eV, C-N and C-O at 286.1 and 286.5 eV respectively [32].

N 1s of the prepared N-GQDs, shown in Fig. 3(c), was fitted into three main peaks at 398, and 402 and 403 eV, attributed mainly to pyrrolic N and graphitic N. The successful nitrogen doping induces redshift in the GQDs PL spectra as detailed in the next section, caused by an electron-doping effect, reducing the magnitude of the electronic gap. The S2p Fig. 3(d) doublet is fitted with two peaks, ascribed to $S2p_{3/2}$ and $S2p_{1/2}$ in the 2:1 ratio.

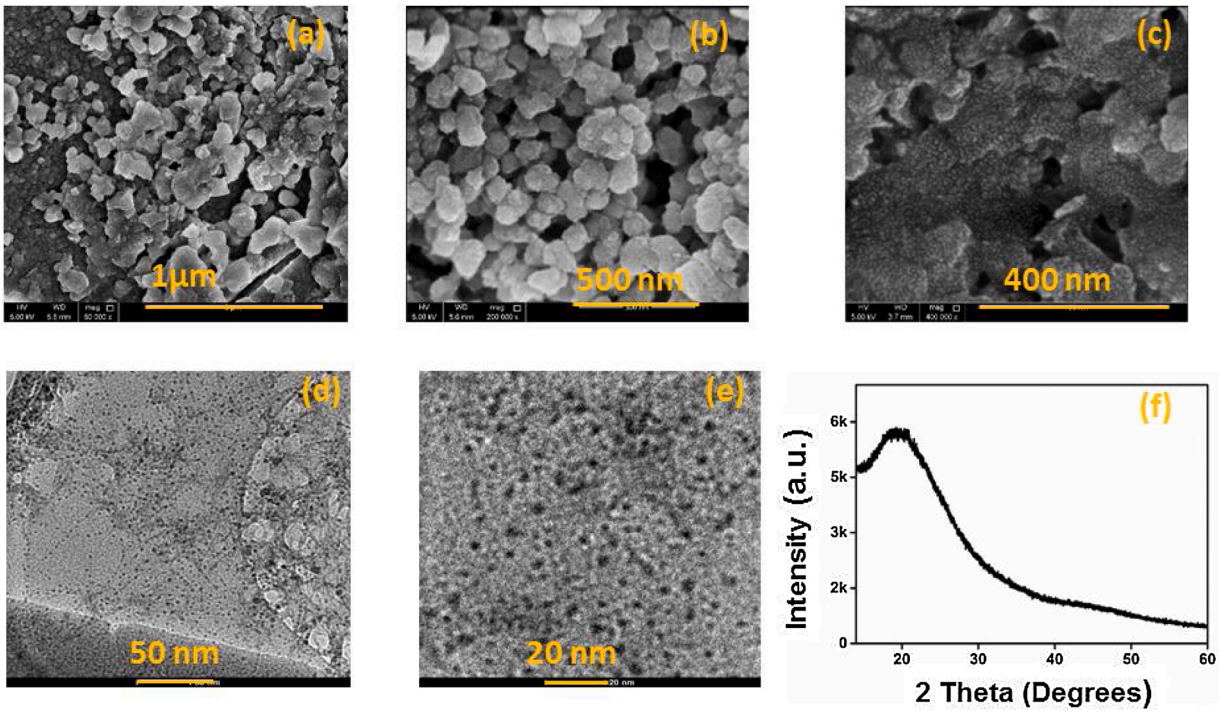

Fig. 6. (a-c) SEM of GQDs on ITO substrate and (d, e) TEM of GQDs at different magnifications, (f) XRD patterns of GQDs.

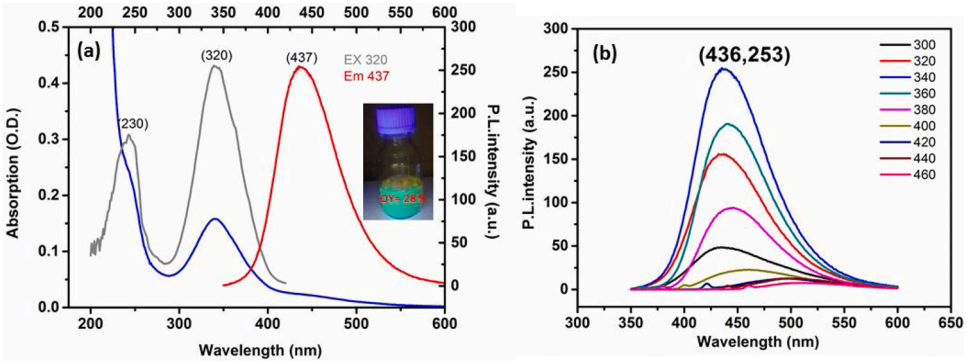

Fig. 7. (a) UV–Vis and PLE absorption spectrum with a digital photograph of fluorescent GQDs under 365 nm UV irradiation, (b) PL excitation-dependent emission spectra of GQDs.

In Fig. 4 (a), the Raman spectra of Graphite waste and N-GQDs are presented. For N-GQDs, the G-band appears at 1593 cm^{-1} and the D-band at 1363 cm^{-1}. The ID/IG value represents a measure of disorder in graphene structure, for graphite waste is 1.36, while for graphite waste, this ratio is 1.06, also suggesting, more disordered carbon structure because of the nitrogen doping effect, blue shifts of D and G bands can be seen, which is consistent with the results reported before [33]. The FTIR spectra of pristine and the as-prepared N-GQDs were displayed in Fig. 4 (b) for graphite and their derivate N-GQDS respectively. One can note two small peaks at 2919 and 2858 cm^{-1}, assigned to $–CH_2$ groups vibration, the band at 3442 cm^{-1} is assigned to –OH group, the peaks at 1608 and 1764 cm^{-1} assigned to C = O groups stretching vibration in carboxylic moiety, the 1440 cm^{-1} peak is due to C–H stretching vibration, while the 1128 cm^{-1} peak could be attributed to C–O stretching vibration. Peaks situated around 1384 and 3153 cm^{-1} are assigned to C-N and N–H stretching vibrations, respectively [34].

Fig. 5 shows the AFM image of N-GQDs derivate from graphite, shows a uniform film (Fig. 5a), the average height of N-GQDs was roughly 2 nm (Fig. 5b), in a range of 1-10 nm, confirming the graphene-like structures in the N-GQDs, as previously described for other GQDs made from carbon sources [35]. The average topographic height was estimated to 0.5 nm (Fig. 5c).

Fig. 6 shows, SEM, TEM, and XRD of the as-prepared GQDs, The SEM of the N-GQDs coated of ITO substrate. The TEM has shown in Fig. 6(d–e) confirmed a monodispersed and uniform spherical structure, high yield, and regular shape and size of the prepared GQDs, with an average size of 10 ± 0.5 nm. The SEM images Fig. 6(a–c) show large particles were grown over the surface of a silicon wafer coated substrate with a spherical shaped and average diameter of grain about100 nm. It was also observed that the GQDs nanoparticles might be converted into bigger clusters due to the agglomeration of a large number of GQDs. The microstructure consists of numerous thin aggregates that are interconnected with each other to form hierarchical displayed uniform surface morphology with spherical shaped grains; as shown in TEM images, it was previously revealed that the Vander Waals forces of solvents caused aggregation of GQDs (between carbon precursors and/or carbon intermediates) and its agglomeration [36, 37]. The XRD analysis of GQDs (Fig. 6f) exhibited a diffraction peak at 2θ at around 27° C, which confirms the graphitic like carbon, facets of the prepared GQDs as previously described [38].

(a)

Sample	2.5 mgGQD-ITO	5 mgGQD-ITO	10 mgGQD-ITO
Contact angle image	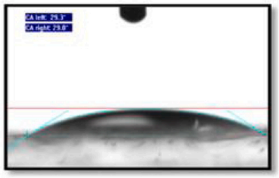	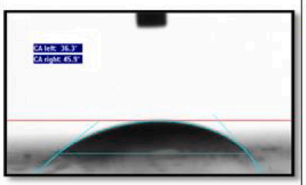	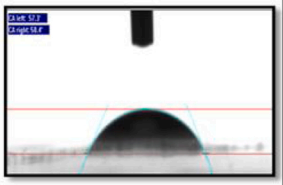
Contact angle	29.15°	41.1°	57.85°

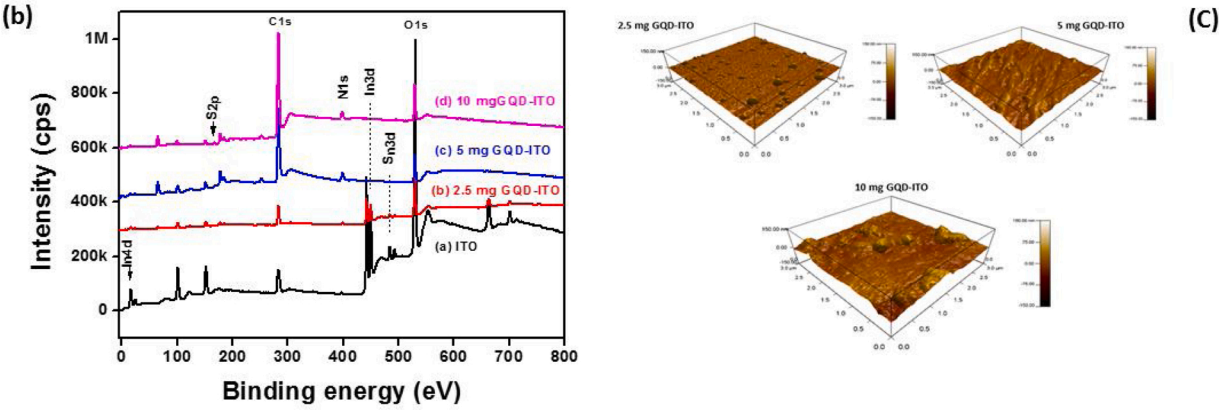

Fig. 8. (a) Contact angle measurements GQDs films using the three different concentrations 2.5 mg, 5 mg, and 10 mg in DMF, (b) XPS spectra of pristine (a), modified GQDs based ITO sensing films(b,c and d), corresponding to 2.5, 5 and 10 mg of added GQDs respectively, (c) AFM image of GQD-ITO 2.5 mg, 5 mg and 10 mg.

3.3. Optical properties of GQDs

UV-vis, PLE and PL spectra of GQDs aqueous solutions were recorded in order to investigate their optical performances (Fig. 7a). From the UV–Vis absorption of the prepared GQDs, one can note two absorption peaks (230 and 320 nm), assigned to π→π* transition of C = C and n→π* transition of C = O, as previously reported for graphene quantum dots based materials [39].

The digital photo of the -prepared GQDs under 365 nm UV light (inset of Fig. 7a), exhibit blue-green color [40]. From the UV data displayed in Fig. 7(a), the bandgap energy of GQDs, was deduced using the equation $[\alpha\upsilon h = A\ (\upsilon h - Eg)^{1/2}]$, where α, υ, h, A, and Eg are the absorption coefficient, light frequency, blank constant, constant, and bandgap energy, respectively. The bandgap of the as-prepared GQDs was increasing to 4.97 eV. This bandgap originated from the doping effect of N and S atoms, as previously reported [41,42]. The Excitation-dependent PL behavior of GQDs using 10 mg concentrations of N-GQDs observed in Fig. 7(b), as previously reported for fluorescent carbon materials prepared from wastes [33]. As shown in Fig. (7b), it was found that with increasing excitation wavelength the intensity of the corresponding emission peak appeared to rise and then to decrease for excitation wavelength larger than 340 nm. The emission with the highest intensity was noted at 437 nm (excited at 340 m). Moreover, the emissions were significantly red-shifted. This phenomenon could be correlated with the aromatic C = C bonds and surface defects resulting from C–OH, C-O, C–S and C–N groups in the GQDs, as previously reported [43]. a blue-green solution with photoluminescence quantum yields PL QY of 28.7% (320 nm excitation) is obtained (320 nm excitation), see Table SI1, in **Supplementary information,** as previously reported[1]

3.4. AFM,XPS and Contact Angle measurements of GQD-ITO with different concentration

Ultrapure water drops were gently deposited on the sensing film surfaces and their contact angles were measured by the sessile drop technique. Fig. 8(a) reports water drop contact angles on GQDs based sensing film, prepared using different GQD concentrations. The contact angle of N-GQDs (2.5 mg) is 29.2° shows, obviously its hydrophilic nature. As the concentration of GQDs increases, the hydrophilicity of the sensing film decreases but remains within the hydrophilic regime; the contact angle of N-GQDs (5 mg) sensing film increased to 41.1° whereas that corresponding to N-GQDs (10 mg) was measured to be 57.9°. The contact angle of 10 mg GQDs film shows that the sensing film remains hydrophilic since the rule of thumb implied that a surface is categorized hydrophilic for water contact angle < 90°. This means that water drops probe both hydrophilic and hydrophobic sites of the surface; the relative global hydrophilic character is in line with enhanced sensitivity of humidity sensors. It is to note that upon addition of GQDs there is hysteresis loss as compared to other used concentrations of N-GQDs (Fig. 8). As we further increase the concentration of GQDs (15 mg), the contact angle measurement shows that sensing film surface becomes more hydrophobic (see Supplementary Material, Figure S1). Hydrophilicity of the as-prepared GQDs based films is due to rich hydrophilic groups such as nitrogen and carboxylic-containing functional groups. Hysteresis significantly decreased for higher initial concentration of GQDs used to make the sensing films. The surface is probably heterogeneous, and ITO XPS signals (Fig. 8b), (In3d and Sn3d core electron level peaks) were detected. Although AFM image in Fig. 8c shows continuous coatings, XPS suggests possible occurrence of In and Sn at the outermost surface due to some sites not fully coated by the dots but which could not be probed by AFM. Further addition of GQDs fills in the voids in the sensing films, hence the complete disappearance of

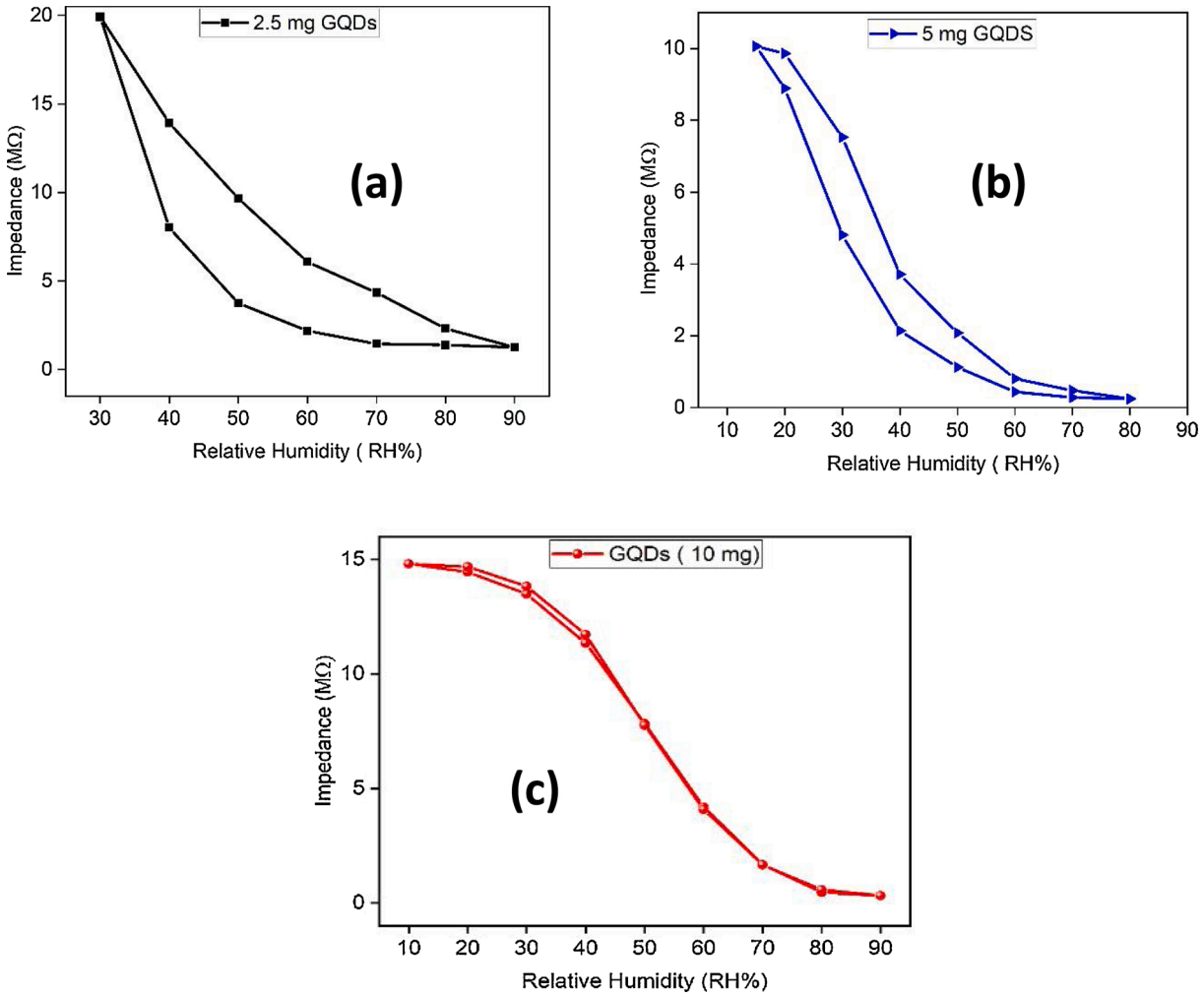

Fig. 9. (a) Hysteresis response of Graphene Quantum dots based resistive humidity sensors operate at 25 ± 1 °C: (a) 2.5 mg GQDS, (b) 5 mg GQDs, and (c) 10 mg GQDs.

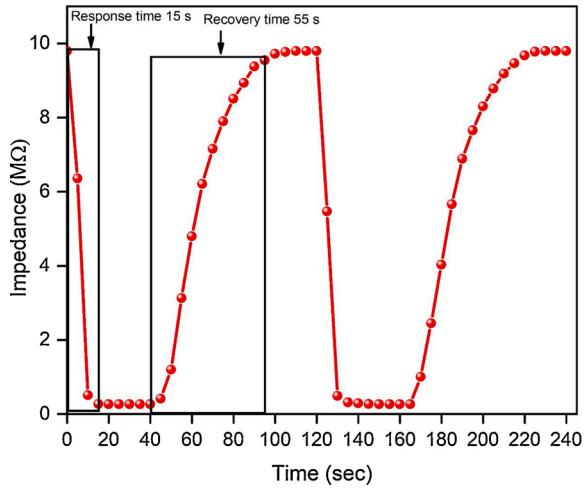

Fig. 10. Response and recovery cycles (40- 90 % RH) of GQDs (10 mg) based resistive humidity sensors response taken at 25 ± 1 °C.

hysteresis. This phenomenon is thus probably due to a combination of morphology and composition. Possible voids induce hysteresis, and hydrophilic functional groups borne by GQDs induce hydrophilic character at any initial concentration of the GQDs.

3.5. Potential humidity sensor application

The N-GQDs based impedance humidity sensors were prepared with different concentrations of N-GQDs (2.5 mg, 5 mg, and 10 mg). The performance of the N-GQDs based impedance humidity sensors was thoroughly investigated. Fig. 8 demonstrates the impedance response of the N-GQDs based resistive humidity sensors, with respect to change in humidity level 10 % RH- 90 % RH. As the humidity level increases within the humidity chamber, more water molecules formed on the surface of the sensing film hence the conductivity of the sensing film also increases. The as-made GQDs with graphene-like structures are rich in oxygen; therefore, water molecules and oxygen radicals would form a strong hydrogen bond; this will increase the hydrophilicity and proton conductivity of the sensing film [44]. Figs. 9a-c show the hysteresis response of the 2.5 mg GQDs, 5 mg GQDs, and 10 mg GQDs based impedance humidity sensors. Hysteresis loss is a significant parameter to evaluate the sensor's performance and sensor stability. The Hysteresis loss can be defined as the maximum shift in impedance when the sensor is subjected to change in relative humidity level from a lower RH level to a higher RH level (absorption process) and higher RH level to lower RH level (desorption process). It was observed from Fig. 8 that at a lower concentration of GQDs (2.5 mg), the impedance humidity sensor shows a higher hysteresis loss. At lower concentrations of GQDs (2.5 mg), sensing film is super hydrophilic; hence the desorption process is slow; therefore, it has higher hysteresis value. As the concentration of GQDs increases, the sensing film becomes less hydrophilic; thus the desorption

Table 1
Comparison of the performance and sensing ranges of different carbon-based humidity sensors.

Material	Experimental details	Sensing Range	Response/Recovery time	Reference
Carbo Carbon Nanotube	• carbon nanotubes are modified with carboxylic groups. • the cellulose used as substrate was coated with COOH-functionalized Carbon Nanotube	10 - 95 %RH	6 s- 120 s	[51]
Reduce graphene oxide/polymer nanocomposite	• Chemically reduced graphene oxide • flexible polyimide used as a substrate • Sensing films were prepared using a layer-by-layer approach	11- 97 %RH	94 s-133 s	[52]
Graphene quantum dots (GQDs)	• Graphene quantum dots (GQDs) were prepared via nanotomy of graphite • GQDs were interfaced with polyelectrolyte microfiber forming electrically percolating network	0 – 40 %RH	NA	[53]
Graphene quantum dots (GQDs) prepared from waste	• Easy hydrothermal method • using graphite waste as a carbon source	40 – 90 %RH	15 s - 55 s	This work

process becomes relatively faster, which reduces the hysteresis value. The hysteresis value for the first two concentrations is a bit higher; however, in the case of the third concentration (10 mg), the maximum hysteresis for the GQDs based impedance humidity sensor is 2.2% at 30 % RH. This value is with the acceptable rage of 3% for the real-life applications of the humidity sensors. The hysteresis value was calculated using the formula given in reference [45].

In order to evaluate the performance of the sensors, response, recovery times, and stability are also considered as essential parameters. The humidity sensor response time has been well described as the time taken by the sensor to reach 90 % RH (in the current study, 40-90 %RH). The recovery time is defined as the time a sensor is required to achieve the initial humidity level (in this case, 40 % RH) from 90 % RH. Fig. 10 illustrates the response and recovery curve of the GQDs (10 mg) based impedance humidity sensor; the curve shows a repeatable and stable response. The response and recovery times of the N-GQDs (10 mg) impedance humidity sensors calculate to be 15 s and 55 s, respectively. Stability test of 10 mg GQDs based impedance humidity sensor (performed over three months). Figure SI2 shows the performance of the sensors with respect to change in humidity levels. The impedance response of GQDs humidity sensors remains stable over the tested time of three months

Indeed, the large surface areas and abundant active N and S sites present on GQDs films can significantly enhance the adsorption and desorption of water molecules [46]. Amino and sulfuric doping groups, present on the surface of GQDs prepared films, introduced nitrogen and sulfur defects [46]. Figure SI3 depicts the adsorption of water molecules on the GQDS based sensing film; at low humidity level, water molecules are first chemisorbed on the sensing film. When the relative humidity level increases, the physisorption of water molecules happens on the chemisorbed surface [47]. Thus more water molecules are physically adsorbed on the two adjacent hydroxyl groups through hydrogen bonding, forming multi-layer water [48]. Due to the presence of amino and sulfuric groups, more hydrogen bonds are generated in the process of continuously binding with water molecules, which is more conducive to the adsorption of water molecules, and the adsorbed water molecules will create protons. Besides, the amino groups are also protonated, and proton hopping is more likely to occur between adjacent water molecules [49]. According to the Grotthuss mechanism, the proton ions can move freely on the GQDs sensing film surface, enhancing the sensing film's ionic conductivity, which increases the sensing film's sensitivity at higher RH levels [50]. Table 1 shows the comparison of our work with previously described carbon-based Humidity sensors. Our newly synthesized material has shown significantly improve the response and recovery times as compared to the previous study.

4. Conclusion

In conclusion, GQDs was successfully prepared from graphite waste via a hydrothermal process in the presence of ammonia. The as-made GQDs with graphene-like structures are fluorescent, rich in oxygen, nitrogen, and sulfur groups, have a uniform size and excellent water solubility. The latter GQDs were used to prepare a resistive humidity sensor using of GQDs. We achieved improved hysteresis (maximum 2.2% at 30 % RH) and stable response. The response and recovery time of the GQDs (10 mg) impedance sensors calculated to be 15 s and 55 s, respectively. This work offers a new way of producing high-quality GQDs from graphite waste to fabricate solid-state materials as an efficient humidity sensor.

CRediT authorship contribution statement

Khouloud Jlassi: Conceptualization, Project administration, Supervision, Validation, Methodology, Data curation, Formal analysis, Writing - original draft. **Shoaib Mallick:** Methodology, Data curation, Formal analysis, Writing - original draft. **Abubaker Eribi:** Methodology. **Mohamed M. Chehimi:** Writing - review & editing. **Zubair Ahmad:** Conceptualization, Project administration, Supervision, Validation, Methodology, Data curation, Formal analysis, Writing - review & editing. **Farid Touati:** Writing - review & editing. **Igor Krupa:** Writing - review & editing.

Declaration of Competing Interest

The authors declare no competing financial interest.

Acknowledgments

This publication was made possible by GSRA3-1-1116-14016 and UREP27-091-2-022 awards from Qatar National Research Fund (a member of Qatar Foundation).from the Qatar National Research Fund (a member of the Qatar Foundation). The others would like to thank the undergraduate students, Miss Doaa Farhan, Mrs. Sayma Salauddin and Ms. Hafsa Mutahir working in frame of UREP27-091-2-022 project the for their assistance in sample preparations and analysis. The findings made herein are solely the responsibility of the authors.

Appendix A. Supplementary data

Supplementary material related to this article can be found, in the online version, at doi:https://doi.org/10.1016/j.snb.2020.129058.

References

[1] J. Dai, H. Zhao, X. Lin, S. Liu, T. Fei, T. Zhang, Design strategy for ultrafast-response humidity sensors based on gel polymer electrolytes and application for detecting respiration, Sensors and Actuators B: Chemical 304 (2020), 127270.
[2] Z. Duan, Q. Zhao, S. Wang, Z. Yuan, Y. Zhang, X. Li, et al., Novel application of attapulgite on high performance and low-cost humidity sensors, Sensors and Actuators B: Chemical 305 (2020), 127534.
[3] H. Yu, C. Wang, F.-Y. Meng, J.-G. Liang, H.S. Kashan, K.K. Adhikari, et al., Design and analysis of ultrafast and high-sensitivity microwave transduction humidity

sensor based on belt-shaped MoO3 nanomaterial, Sensors and Actuators B: Chemical 304 (2020), 127138.
[4] B. Chethan, H.R. Prakash, Y. Ravikiran, S. Vijayakumari, S. Manjunatha, S. Thomas, Humidity sensing performance of hybrid nanorods of polyaniline-Yttrium oxide composite prepared by mechanical mixing method, Talanta (2020), 120906.
[5] X. Yu, X. Chen, X. Ding, X. Chen, X. Yu, X. Zhao, High-sensitivity and low-hysteresis humidity sensor based on hydrothermally reduced graphene oxide/nanodiamond, Sensors and Actuators B: Chemical 283 (2019) 761–768.
[6] J. Dai, T. Zhang, H. Zhao, T. Fei, Preparation of organic-inorganic hybrid polymers and their humidity sensing properties, Sensors Actuators B: Chem 242 (2017) 1108–1114.
[7] C. Lv, C. Hu, J. Luo, S. Liu, Y. Qiao, Z. Zhang, et al., Recent advances in graphene-based humidity sensors, Nanomaterials 9 (2019) 422.
[8] M.S. Mauter, M. Elimelech, Environmental applications of carbon-based nanomaterials, Environmental Science & Technology 42 (2008) 5843–5859.
[9] D. Zhang, X. Zong, Z. Wu, Fabrication of tin disulfide/graphene oxide nanoflower on flexible substrate for ultrasensitive humidity sensing with ultralow hysteresis and good reversibility, Sensors and Actuators B: Chemical 287 (2019) 398–407.
[10] H. Sun, L. Wu, W. Wei, X.J.M.t. Qu, Recent advances in graphene quantum dots for sensing, 16(2013) 433-442.
[11] H. Sun, L. Wu, W. Wei, X. Qu, Recent advances in graphene quantum dots for sensing, Materials today 16 (2013) 433–442.
[12] X. Zhao, W. Gao, H. Zhang, X. Qiu, Y. Luo, Graphene quantum dots in biomedical applications: recent advances and future challenges, Handbook of Nanomaterials in Analytical Chemistry, Elsevier, 2020, pp. 493–505.
[13] R. Aacharya, H. Chhipa, Nanocarbon fertilizers: Implications of carbon nanomaterials in sustainable agriculture production, Carbon Nanomaterials for Agri-Food and Environmental Applications, Elsevier, 2020, pp. 297–321.
[14] L. Cao, K. Shiral Fernando, W. Liang, A. Seilkop, L. Monica Veca, Y.-P. Sun, et al., Carbon dots for energy conversion applications, Journal of Applied Physics 125 (2019), 220903.
[15] H. Ouarrad, F.-Z. Ramadan, L. Drissi, Size engineering optoelectronic features of C, Si and CSi hybrid diamond-shaped quantum dots, RSC Advances 9 (2019) 28609–28617.
[16] S. Shen, B. Huang, X. Guo, H. Wang, A dual-responsive fluorescent sensor for Hg 2 + and thiols based on N-doped silicon quantum dots and its application in cell imaging, Journal of Materials Chemistry B 7 (2019) 7033–7041.
[17] H. Elmizadeh, M. Soleimani, F. Faridbod, G. Bardajee, Fabrication of a nanomaterial-based fluorescence sensor constructed from ligand capped CdTe quantum dots for ultrasensitive and rapid detection of silver ions in aqueous samples, Spectrochimica Acta Part A: Molecular and Biomolecular Spectroscopy 211 (2019) 291–298.
[18] M. Bilal, E. Oh, R. Liu, J.C. Breger, I.L. Medintz, Y. Cohen, Bayesian Network Resource for Meta-Analysis: Cellular Toxicity of Quantum Dots, Small 15 (2019), 1900510.
[19] J.C. Kays, A.M. Saeboe, R. Toufanian, D.E. Kurant, A.M. Dennis, Shell-Free Copper Indium Sulfide Quantum Dots Induce Toxicity in Vitro and in Vivo, Nano Letters 20 (2020) 1980–1991.
[20] M. Wu, Y. Wang, W. Wu, C. Hu, X. Wang, J. Zheng, et al., Preparation of functionalized water-soluble photoluminescent carbon quantum dots from petroleum coke, Carbon 78 (2014) 480–489.
[21] V. Ruiz, I. Fernández, P. Carrasco, G. Cabañero, H.J. Grande, J. Herrán, Graphene quantum dots as a novel sensing material for low-cost resistive and fast-response humidity sensors, Sensors and Actuators B: Chemical 218 (2015) 73–77.
[22] S. Iravani, R.S. Varma, Green synthesis, biomedical and biotechnological applications of carbon and graphene quantum dots. A review, Environmental Chemistry Letters (2020) 1–25.
[23] S. Lai, Y. Jin, L. Shi, R. Zhou, Y. Zhou, D. An, Mechanisms behind excitation-and concentration-dependent multicolor photoluminescence in graphene quantum dots, Nanoscale 12 (2020) 591–601.
[24] X. Yan, B. Li, X. Cui, Q. Wei, K. Tajima, L.-s. Li, Independent tuning of the band gap and redox potential of graphene quantum dots, The journal of physical chemistry letters 2 (2011) 1119–1124.
[25] C. Hu, Y. Liu, Y. Yang, J. Cui, Z. Huang, Y. Wang, et al., One-step preparation of nitrogen-doped graphene quantum dots from oxidized debris of graphene oxide, Journal of Materials Chemistry B 1 (2013) 39–42.
[26] Y. Zhang, M. Park, H.Y. Kim, B. Ding, S.-J. Park, A facile ultrasonic-assisted fabrication of nitrogen-doped carbon dots/BiOBr up-conversion nanocomposites for visible light photocatalytic enhancements, Scientific reports 7 (2017) 1–12.
[27] W. Li, M. Li, Y. Liu, D. Pan, Z. Li, L. Wang, et al., Three minute ultrarapid microwave-assisted synthesis of bright fluorescent graphene quantum dots for live cell staining and white LEDs, ACS Applied Nano Materials 1 (2018) 1623–1630.
[28] S. Kang, Y.K. Jeong, J.H. Ryu, Y. Son, W.R. Kim, B. Lee, et al., Pulsed laser ablation based synthetic route for nitrogen-doped graphene quantum dots using graphite flakes, Applied Surface Science 506 (2020), 144998.
[29] D.B. Shinde, V.K. Pillai, Electrochemical preparation of luminescent graphene quantum dots from multiwalled carbon nanotubes, Chemistry–A European Journal 18 (2012) 12522–12528.
[30] L. Li, D. Liu, K. Wang, H. Mao, T. You, Quantitative detection of nitrite with N-doped graphene quantum dots decorated N-doped carbon nanofibers composite-based electrochemical sensor, Sensors and Actuators B: Chemical 252 (2017) 17–23.
[31] A. Pourjavadi, H. Abdolmaleki, M. Doroudian, S.H. Hosseini, Novel synthesis route for preparation of porous nitrogen-doped carbons from lignocellulosic wastes for high performance supercapacitors, Journal of Alloys and Compounds 827 (2020), 154116.
[32] Y. Li, Y. Zhao, H. Cheng, Y. Hu, G. Shi, L. Dai, et al., Nitrogen-doped graphene quantum dots with oxygen-rich functional groups, Journal of the American Chemical Society 134 (2012) 15–18.
[33] K. Jlassi, K. Eid, M.H. Sliem, A.M. Abdullah, M.M. Chehimi, I. Krupa, Rational synthesis, characterization, and application of environmentally friendly (polymer–carbon dot) hybrid composite film for fast and efficient UV-assisted Cd 2 + removal from water, Environmental Sciences Europe 32 (2020) 1–13.
[34] J. Jiang, Y. He, S. Li, H. Cui, Amino acids as the source for producing carbon nanodots: microwave assisted one-step synthesis, intrinsic photoluminescence property and intense chemiluminescence enhancement, Chemical communications 48 (2012) 9634–9636.
[35] H. Fei, R. Ye, G. Ye, Y. Gong, Z. Peng, X. Fan, et al., Boron-and nitrogen-doped graphene quantum dots/graphene hybrid nanoplatelets as efficient electrocatalysts for oxygen reduction, ACS Nano 8 (2014) 10837–10843.
[36] Y. Dong, J. Lin, Y. Chen, F. Fu, Y. Chi, G. Chen, Graphene quantum dots, graphene oxide, carbon quantum dots and graphite nanocrystals in coals, Nanoscale 6 (2014) 7410–7415.
[37] K. Hagiwara, H. Uchida, Y. Suzuki, T. Hayashita, K. Torigoe, T. Kida, et al., Role of alkan-1-ol solvents in the synthesis of yellow luminescent carbon quantum dots (CQDs): van der Waals force-caused aggregation and agglomeration, RSC Advances 10 (2020) 14396–14402.
[38] S. Gu, C.-T. Hsieh, C.-Y. Yuan, Y.A. Gandomi, J.-K. Chang, C.-C. Fu, et al., Fluorescence of functionalized graphene quantum dots prepared from infrared-assisted pyrolysis of citric acid and urea, Journal of Luminescence 217 (2020), 116774.
[39] Z. Zhang, J. Zhang, N. Chen, L. Qu, Graphene quantum dots: an emerging material for energy-related applications and beyond, Energy & Environmental Science 5 (2012) 8869–8890.
[40] R. Ye, C. Xiang, J. Lin, Z. Peng, K. Huang, Z. Yan, et al., Coal as an abundant source of graphene quantum dots, Nature communications 4 (2013) 2943.
[41] X. Li, S.P. Lau, L. Tang, R. Ji, P. Yang, Multicolour light emission from chlorine-doped graphene quantum dots, Journal of Materials Chemistry C 1 (2013) 7308–7313.
[42] B. Rajbanshi, S. Sarkar, P. Sarkar, Band gap engineering of graphene–CdTe quantum dot hybrid nanostructures, Journal of Materials Chemistry C 2 (2014) 8967–8975.
[43] S. Sarkar, M. Sudolska, M. Dubecky, C.J. Reckmeier, A.L. Rogach, R. Zboril, et al., Graphitic nitrogen doping in carbon dots causes red-shifted absorption, The Journal of Physical Chemistry C 120 (2016) 1303–1308.
[44] L. Guo, H.-B. Jiang, R.-Q. Shao, Y.-L. Zhang, S.-Y. Xie, J.-N. Wang, et al., Two-beam-laser interference mediated reduction, patterning and nanostructuring of graphene oxide for the production of a flexible humidity sensing device, Carbon 50 (2012) 1667–1673.
[45] A. Tripathy, S. Pramanik, A. Manna, S. Bhuyan, N.F. Azrin Shah, Z. Radzi, et al., Design and development for capacitive humidity sensor applications of lead-free Ca, Mg, Fe, Ti-oxides-based electro-ceramics with improved sensing properties via physisorption 16 (2016) 1135.
[46] W. Meng, S. Wu, X. Wang, D. Zhang, High-sensitivity resistive humidity sensor based on graphitic carbon nitride nanosheets and its application, Sensors and Actuators B: Chemical 315 (2020), 128058.
[47] Y. Zhang, H. Zou, J. Peng, Z. Duan, M. Ma, X. Xin, et al., Enhanced humidity sensing properties of SmFeO3-modified MoS2 nanocomposites based on the synergistic effect, Sensors and Actuators B: Chemical 272 (2018) 459–467.
[48] J. Xie, H. Wang, Y. Lin, Y. Zhou, Y. Wu, Highly sensitive humidity sensor based on quartz crystal microbalance coated with ZnO colloid spheres, Sensors and Actuators B: Chemical 177 (2013) 1083–1088.
[49] H. Dai, N. Feng, J. Li, J. Zhang, W. Li, Chemiresistive humidity sensor based on chitosan/zinc oxide/single-walled carbon nanotube composite film, Sensors and Actuators B: Chemical 283 (2019) 786–792.
[50] N. Agmon, The grotthuss mechanism, Chemical Physics Letters 244 (1995) 456–462.
[51] J.-W. Han, B. Kim, J. Li, M. Meyyappan, Carbon nanotube based humidity sensor on cellulose paper, The Journal of Physical Chemistry C 116 (2012) 22094–22097.
[52] D. Zhang, J. Tong, B. Xia, Humidity-sensing properties of chemically reduced graphene oxide/polymer nanocomposite film sensor based on layer-by-layer nano self-assembly, Sensors and Actuators B: Chemical 197 (2014) 66–72.
[53] T. Sreeprasad, A.A. Rodriguez, J. Colston, A. Graham, E. Shishkin, V. Pallem, et al., Electron-tunneling modulation in percolating network of graphene quantum dots: Fabrication, phenomenological understanding, and humidity/pressure sensing applications, Nano letters 13 (2013) 1757–1763.

Dr. Jlassi Khouloud is a researcher at the Center of Advanced Materials (CAM) Qatar University. She is a doctor in chemistry from the Paris Diderot (ITODYS) lab in the “chemistry of materials and functional surfaces.” She is involved in the interface chemistry of nanoclay using either silanes or diazonium salts bearing polymerization initiator groups or polymer; recently, she is working on Carbon and graphene quantum dots for water treatment, energy conversion, and new applications. Dr. Khouloud has published many papers in international peer-reviewed journals in the area of applied clay-polymer nano-composites. Previously, she was working as an assistant professor in the higher institute of environmental science and technologies in Tunisia for four years.

Shoaib Mallick received his M.S. degree in Wireless and Photonics Engineering from Chalmers University of Technology, Sweden, in 2012. He joined Texas A&M University at

Qatar as a Research Associate to work on oil and gas sensing project from May1,2013 to October 31, 2014. He was awarded Graduate Sponsorship Research Award (GSRA) from Qatar Foundation in February 2016 for pursuing his Ph.D. degree in Electrical Engineering at Qatar University, Doha, Qatar. He has published research articles in reputed journals and international conferences. His research work focused in the area of polymer and ferroelectric materials for sensors and resonator applications.

Abubaker Eribi is an undergraduate student at the department of chemical engineering, college of engineering, Qatar University.

Mohamed M. Chehimi Mohamed M. Chehimi is the Research Director at French CNRS. He obtained a Ph.D. in Physical Organic Chemistry at the University Paris Diderot in 1988 and joined CNRS in 1989 for a permanent researcher position. He was promoted Research Director Grade 1 (DR1) in 2011. His research topics include the design of reactive and functional polymer and nanocomposite coatings. In recent years he has spent time and effort developing aryldiazonium salts as new coupling agents in materials science. The applications encompass adsorbents, electrochemical sensors, fillers, antibacterial surfaces, and electronic devices. He is also a specialist in XPS analysis of a broad range of materials, including polymer composites. He has published over 250 research papers and 20 book chapters. He is the editor of three books and guest-edited three themed issues. He has supervised over 20 Ph.D. theses and collaborated with academic researchers from 15 countries.

Zubair Ahmad is leading the "Materials for Energy and Sustainable Environment, MESE" research group at Center for Advanced Materials (CAM), Qatar University, Doha, Qatar. He received his M.S. degree (Engineering Sciences) in 2008 from Ghulam Ishaq Khan Institute of Engineering Sciences and Technology, Pakistan, and Ph.D. degree (Applied Physics) in 2011 from the same institute. He has over five years of research experience at Mechatronic Research Group, Department of Mechanical Engineering, University of Auckland New Zealand, INHA University South Korea, and the University of Malaya before joining Qatar University. His area of research includes sensors and sustainable energy materials.

Farid Touati received his B.Sc. in Electrical Engineering, Monastir College of Engineering, ENIM, Tunisia (1988) and M.S. in Electrical Engineering Nagoya Institute of Technology, Nagoya, Japan, 1992. He received his Ph.D. in Electrical Engineering from Nagoya Institute of Technology, Nagoya, Japan, 1995. He has over 20 years' experience in industrial electronics. He is working as an Associate Professor in Qatar University. He has over 20 years' experience in industrial electronics. He has more 200 papers and several books/book chapters. He is carrying 7 QNRF research grants (worth $8.0 million). He was involved in NSF--EPSCoR/NSF 00--43 Grant, Alabama Research Infrastructure on "Integrated MEMS Photonics for Computer and Communication Systems: develop new integrated MEMS photonic devices and optical interconnection for parallel processing systems", 2001-2004. His principle area of research includes Sensors, Embedded system design, Biomedical systems (u-healthcare), Organic electronics.

Igor Krupa QAPCO Polymer Chair Professor at Center for Advanced Materials (CAM) Qatar University.